Phys. Status Solidi B **253,** No. 8, 1629–1637 (2016) / **DOI** 10.1002/pssb.201552683

physica status solidi b
www.pss-b.com
basic solid state physics

Can a benign *j–V* characteristic with current saturation be the beginning of a new area of semiconductor physics? The vanishing space charge cleans up the defect-level spectrum

Karl W. Böer*

University of Delaware, Physics and Astronomy, Professor emeritus, 138 Moorings Park Drive, O301, Naples, Florida 34105, USA

Received 26 October 2015, revised 25 February 2016, accepted 8 March 2016
Published online 26 April 2016

Keywords CdS, high-field domains, hole injection, quasi-Fermi levels, space charge, work function

* e-mail solpax@aol.com; karlwboer@gmail.com, Phone: 239-290-2424, Fax: 239-530-2425

The measurement of the current as a function of the applied voltage is a primary tool to investigate the electrical properties and much attention was given to its deviation from ohmicity. Only recently we have learned that even the most simple characteristics with saturation current can be full of surprises. In this paper, we will emphasize how important it is to employ immediately other tools, such as the Franz–Keldysh effect to make the field distribution visible. We will very briefly review the electrode-adjacent high-field domain and their ability to render a CdS crystal thermodynamically stable as being n- or p-type, i.e., being ambipolar depending on whether the domain is attached to the cathode or anode, respectively. We will now also point to the differences for junction-adjacent high-field domains. We will focus on the small slab between a blocking contact and a high-field domain that permits a precise spread of the quasi-Fermi levels within the domains. Within the domains, the crystal is space-charge-free and permits to investigate the electronic transitions to defect levels around the quasi-Fermi levels. The defect levels are free from distortion caused by electric field variation in their neighborhood caused by space charges. A very steep electron quenching minimum is shown in the p-type CdS with anode-adjacent domain. The domains are stabilized by the electron density at blocking cathodes and by hole densities at blocking anodes.

1 Introduction The current–voltage characteristic has always been a primary means to investigate the electronic behavior of photoconductivity, as given in two examples for the model substance [1] CdS in Figs. 1 and 2.

For a large range of optical generation between these two figures and for copper-doped CdS with blocking contacts one observes characteristics as shown in Fig. 3 that show current saturation over a large range of applied voltages with no market features.

These characteristics are obtained with stationary electrode-adjacent high-field domains that do not signalize their existence except for a field distribution-probing that is most easily done by Franz–Keldysh effect observation.

1.1 The high-field domains The high-field domains are characteristic field inhomogeneities in semiconductors when at higher applied voltages, the current decreases steeper than linearly with the electric field, then suddenly a region of high field is introduced (the high-field domain) and the current remains constant with increased bias. These domains have created a large theoretical and technical interest.

1.2 The Schöll and the Böer domains When the high-field domains disattach themselves from the electrodes they move and make themselves known by current oscillations or fluctuations and prompted hundreds of publications and dozens of books [2]. Shortly after Ulrich Kümmel discovered these domains in our Laboratory in 1958 [3], Ekkehard Schöll explained them correctly first with his coworkers at the TU Berlin. I will take this opportunity to propose the name "Schöll domains" for all moving domains that I already proclaimed in a recent

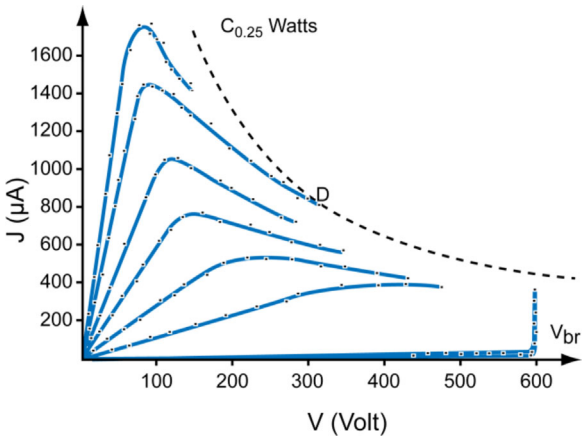

Figure 1 *j–V* characteristic for CdS with light intensity as family parameter, showing some field quenching.

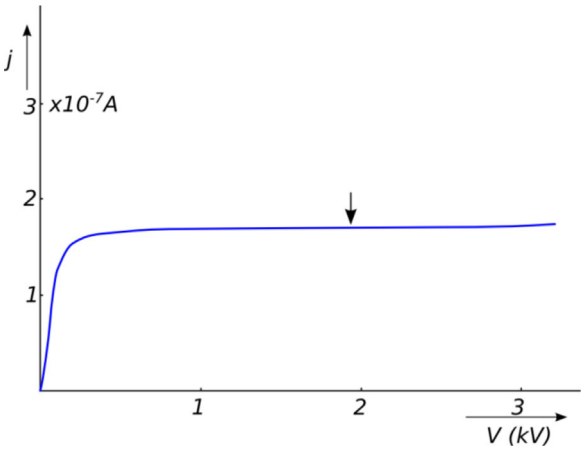

Figure 3 *j–V* characteristic of a copper-doped CdS crystal with gold slit contacts and two electrode-adjacent high-field domains. The arrow indicates the transition from cathode- to anode-adjacent domain and from n- to p-type conductivity in an ambipolar CdS as will be explained below in much more detail.

invited paper that I gave at the Department of Solid State Physics of the Technical University of Berlin on October 13. This proposal is in deviation of the name that was given to me a few years ago [4] and I will no longer accept for moving domains, but restrict the name "Böer" domains solely for stationary domains that attach to electrodes or junctions. We will now present a short review of electrode-attached high-field domains.

2 Cathode-adjacent high-field domain High-field domains are commonly discussed as the projection of the solution of the transport and Poisson equations in a field-of direction diagram [5] (Fig. 4) that shows the electron neutrality curve (red) for which $dn/dx = 0$ and the drift current curve (blue) for which $dF/dx = 0$. The solution curve (a) stars at the boundary concentration n_c and arrives at the singular point when it flattens out in the bulk. When with increased applied voltage the drift curve is shifted to the right (b), it can again intersect the neutrality curve when it is steeply enough decreasing because of field quenching. If this intersection coincides with the boundary density of a blocking cathode (Au) n_c, a new singular point II occurs, the solution flattens again and the high-field domain is created.

The high-field domains can be easily observed by shining light through the CdS platelet [6] (Fig. 5) at the absorption edge and the domain becomes visible as darkened region (see Fig. 6).

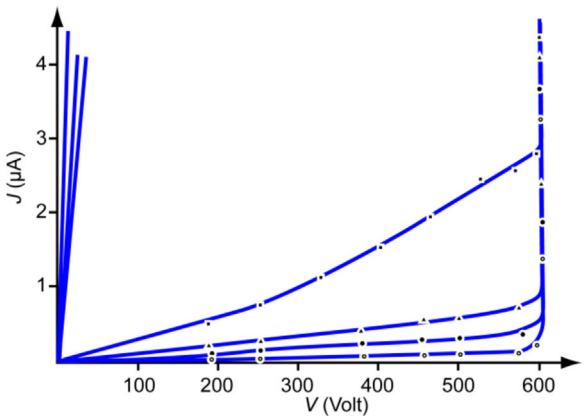

Figure 2 Same as Fig. 1 but for lower light intensities showing slight electron excitation from traps at the higher intensity with an upward bending.

2.1 The second thermodynamically stable conductivity state of CdS These domains are stabilized by the electron concentration at the Schottky barrier n_c and

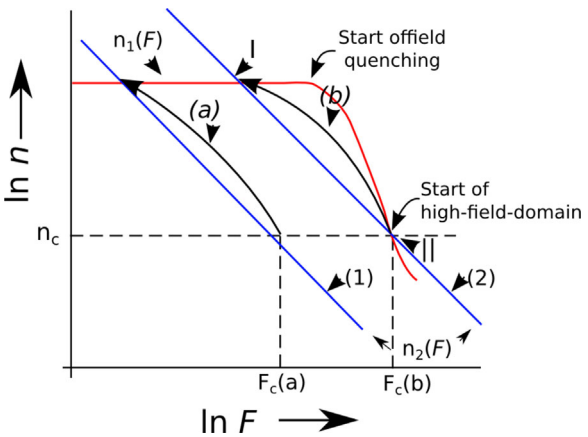

Figure 4 Field-of-direction with the solution curve of a typical Schottky barrier shown as (a). With field quenching the neutrality curve starts to decrease, and when it decreases stronger than linearly, it can intersect again with the drift current curve $n_2(F)$, when, with increased applied voltage it is shifted to the right (curve 2). It causes a second singular point II at which $dn/dx = dF/dx = 0$ it intersects with the Schottky boundary concentration n_c. Then the resulting solution curve flattens out, the field remains constant near (for detail see Section 3) the metal/semiconductor contact and a the high-field domain (b) is formed.

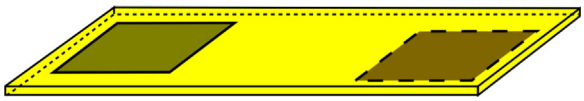

Figure 5 Electrode arrangement on opposite sides to avoid glide discharges at higher bias.

need no external resistance for stabilization: that is, with slight variation in external conditions (bias, temperature, or optical excitation) they return to their thermodynamic stable condition. This indicates that the shown field-quenched state within the domain is free of space-charge and is a second thermodynamically stable state of the conductivity of CdS that is now at higher electric fields [7].

3 Anode-adjacent ultra-high-field domains When extending the neutrality curve in the field-of-direction, it will reach a field range in which field quenching has reached its maximum value and the $n_1(F)$ curve starts to increase again, as shown in Fig. 7. This causes a third singular point (III) to occur by intersecting $n_1(F)$ and $n_2(F)$ again [8].

3.1 Transition between the two types of stationary domains At this transition, an abrupt change of the direction of the solution (green curve in Fig. 7) is observed: the anode has moved from the singular point II to the singular point III.

At the transition point, the original cathode-adjacent high-field domain has filled the entire crystal, the solution has now degenerated to be contained within the singular point II and is constant in $n(x)$ and $F(x)$ throughout the entire CdS. When the applied voltage is increased, the drift field curve moves very slightly above II, the direction of the solution flips, and the starting position of $p(F)$ flips to p_A(Fig. 8) but the solution appears essentially "pinned" near II, that is "at" n_c. It can only move up when the crystal is

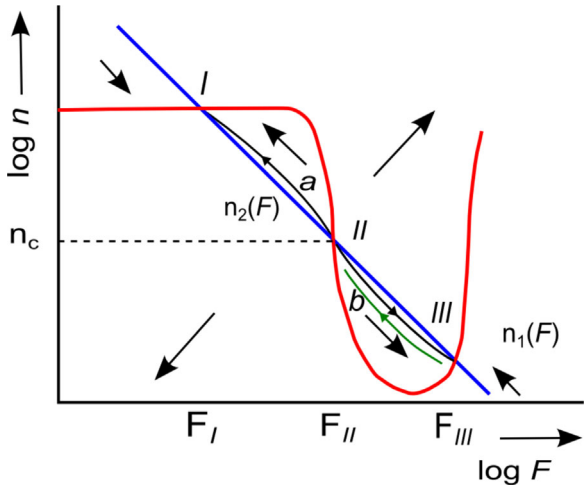

Figure 7 Field-of-direction diagram as in Fig. 6, but now extending to higher fields, exposing another singular point III at the third intersection of $n_1(F)$ and $n_2(F)$. Curve a represents the cathode-adjacent domain, curve b represents an anode-adjacent domain (observe the changing directions of the arrows of a and b: the end-points of the electron current arrows indicate the "attachment points" of the domains, i.e.. the cathode and the anode. We have shown this by a green arrow b, indicating that the current is now carried by holes – see below).

again entirely filled by the anode-adjacent domain – here the dielectric breakdown range starts.

3.2 Observation of cathode and anode-adjacent domains in the same crystal This transition from cathode- to anode-adjacent domain is observed using the Franz–Keldysh effect as is shown in Fig. 6. The cathode is at the left, the anode at the right; they are evaporated with gold at the edges [10] of the CdS. During the entire transition from cathode- to anode-adjacent domain the current remains

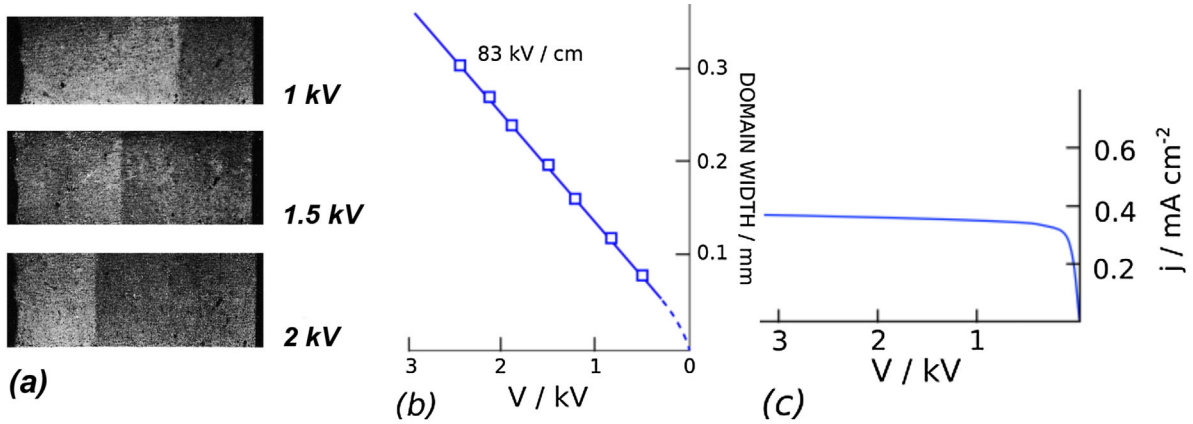

Figure 6 (a) High-field domain seen as darkened region extending from the cathode at the right and extending in width with increasing applied voltage, given at the right edge; (b) width of the domain as a function of the applied voltage showing the slope of 83 kV cm^{-1} as the domain field, and (c) current–voltage characteristics showing current saturation during the entire extend of the cathode-adjacent domain [5].

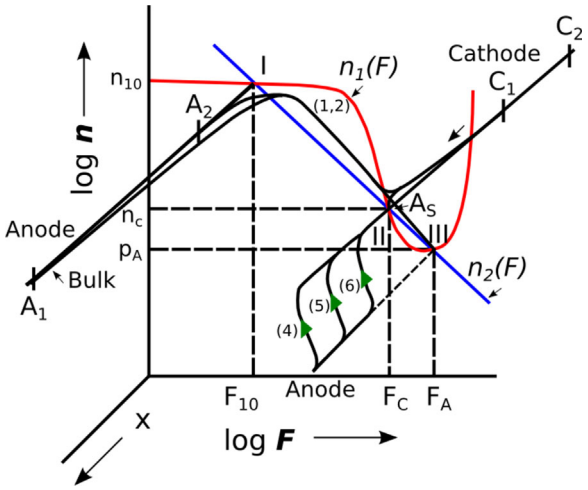

Figure 8 Quasi-three-dimensional [9] rendering of the solution curve with the electron-blocking cathode n_c and the hole blocking p_A identified, and the dynamic of the anode-adjacent domain shown coming out from the anode and expanding toward the cathode. A_s identifies the singular point solution (3) where the entire crystal has constant field and carrier density.

constant (Fig. 9b). Such transition would be completely obscured in the conventional *j–V* analysis.

The band model of the domains is given in Fig. 10a for the cathode-adjacent and in Fig. 10b for the anode-adjacent domain.

Within the domains the CdS is space-charge-free except for the small transition region between both domains where space charges accommodate the changes of the electric fields.

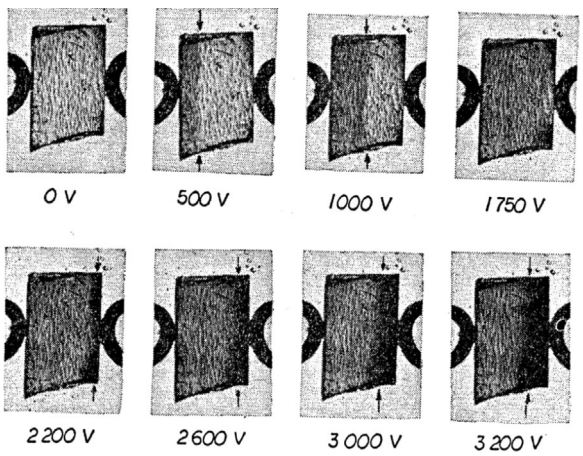

Figure 9 Cathode-adjacent domain extending from 500 to 1750 V bias, then filling the entire crystal. When increasing the bias further, a new high-field domain starts from the anode at about 2 kV as shown in the lower row of photos and extends in width with increased bias. The super-high-field domain has a substantially higher field, as indicated by the increased density of the domain picture. The fact that the anode-adjacent super-high-field domain increases in width from anode toward the cathode already identifies it as a hole depletion and not an electron depletion domain. The arrows above and below the photos indicate the edges of the domain.

3.3 Benign *j–V* characteristic with current saturation From the slope of the domain width with bias one obtains 80 kV cm^{-1} for the field in the cathode-adjacent domain, and 135 kV cm^{-1} for the anode-adjacent domain (see Fig. 11a).

We like to emphasize that during the transition from the cathode-adjacent to the anode-adjacent domain, the current remains saturated without a break visible in the characteristic, since the minute shift of the drift current curve from below to above the singular point II is not detectable (Fig. 11b).When observing such characteristic that fits well within the set of characteristics shown in Figs. 1 and 2, nobody would have expected that something so special has occurred, if it would not be for the observation of electrode-adjacent high-field domains using the Franz–Keldysh effect and their usefulness as will be described in the following sections. Obviously CdS has ambipolar conductivity, its n-type dominates left of the arrow and its p-type right of the arrow.

3.4 The third thermodynamically stable conductivity state of CdS The anode-adjacent high-field domain turned the CdS into a p-type semiconductor that is stabilized by the limited supply of holes from the blocking anode. This state is space-charge free and carried by hole drift only; it is totally stable, that is, when external conditions like temperature, optical excitation, or applied voltage are slightly changed, it returns to the original state.

3.5 The junction-adjacent high-field domains When a thin layer of copper-doped CdS is adjacent to a pn-junction of a p-type solar cell, e.g., a CdTe cell, the high-field domain begins to develop, starting from the junction as soon as the field is strong enough to cause major field quenching. This is on the order of 30 kV cm^{-1} typically achieved close to the junction on the CdS side of a CdS/CdTe solar cell. With shifting reverse bias, the field in the domain increases further until it becomes limited by the Richardson–Dushman diffusion current [11] from the CdTe when the solar cell saturation current is reached. Now the junction adjacent high-field domain is fully developed and is space-charge-free. It is carried by hole drift current alone.

With a current density of $j_{sc} = 24$ mA cm^{-2} and a hole mobility of 30 cm^2/Vs, and an estimated field in the domain of 100 kV cm^{-1} one estimates a hole density in the domain of $p(\mathrm{CdS}) = 5 \times 10^{10}$ cm^{-3}. This causes the Debye length $L_D = 1{,}205[\varepsilon_{stat} T \times 10^{15}/(10 \times 300p)]^{1/2}$ Å $=$ 15,000 μm. This is much larger than the thickness of 200 Å of the CdS, and forces the transition from the high-field domain directly into the boundary layer of the metal contact. This connection is very short within a few Angstroms and contains the image force to establish the work function of the metal [7]. The hole current is consequently carried

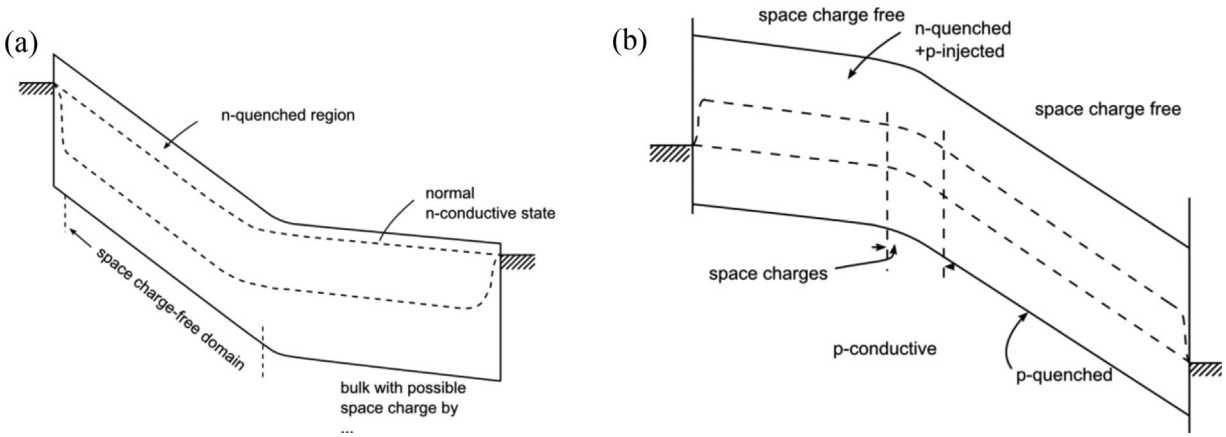

Figure 10 (a) Cathode-adjacent high-field domain, CdS is n-type. (b) Anode-adjacent high-field domain, CdS has turned p-type.

directly from the CdTe solar cell into the n-blocking electrode by tunneling without additional losses.

Unfortunately the CdS layer is too thin to permit directly observation of the extent of the high-field domain. Therefore, we must resort to an estimate of the possible field that we have obtained from many other platelets at different doping and optical excitation and found it for anode-adjacent domains in the range of 90–125 $\mathrm{kV\,cm^{-1}}$ undefined. Therefore, we assume a field of 100 $\mathrm{kV\,cm^{-1}}$ for the domain in the 200 Å thick copper-doped CdS layer.

With these information we now have the basis to draw a to scale model of the CdS/CdTe solar cell [12].

3.6 Consequences for the band model of the CdS/CdTe solar cell [13] Since the conductivity in the CdS with the junction-adjacent high-field domain is p-type, its hole density is expressed by drift, with a current density of $j_{sc} = 24\,\mathrm{mA\,cm^{-2}}$ and a hole mobility of $30\,\mathrm{cm^2\,Vs^{-1}}$, and an estimated field in the domain of $100\,\mathrm{kV\,cm^{-1}}$ one estimates a hole density in the domain of $p(\mathrm{CdS}) = 5 \times 10^{10}\,\mathrm{cm^{-3}}$ or the distance of the quasi-Fermi level from the valence band of $E_{Fp} - E_v = 0.48\,\mathrm{V}$.

In CdTe the hole current [14] at the junction interface is diffusion-limited:

$$j_{sc} = e v_p^* p,$$

with the limiting Richardson–Dushman diffusion current velocity given by

$$v_p^* = \left(3kT/m_p\right)^{1/2} = 1.2 \times 10^7\,\mathrm{cm\,s^{-1}},$$

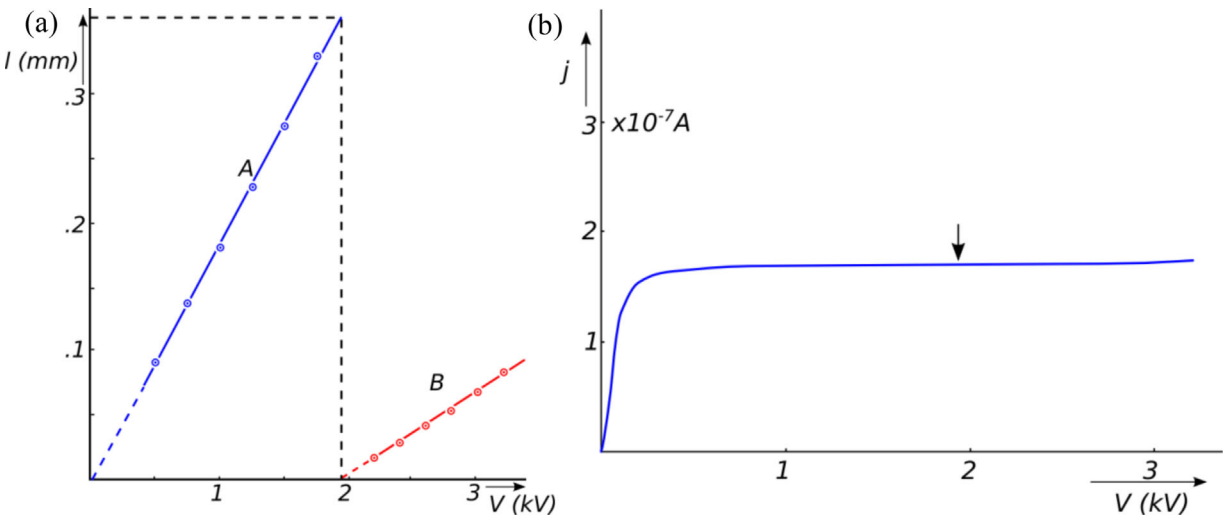

Figure 11 (a) Domain width as a function of the applied voltage for the cathode-adjacent (A) and for the anode-adjacent domain (B). The current–voltage characteristic shown in (b) is taken from the same crystal. During the transition from cathode- to anode-adjacent domain the current remains constant with no break; the arrow indicates the transition point.

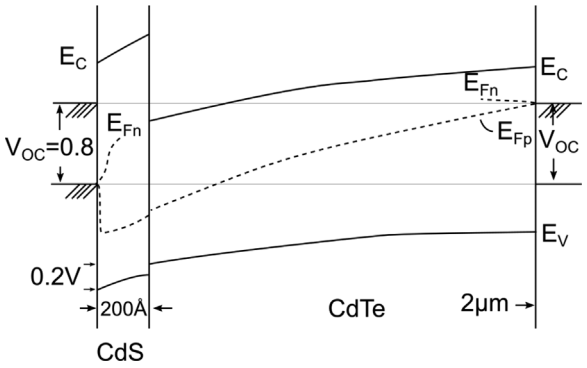

Figure 12 To-scale band model of the CdS/CdTe solar cell. The missing continuation of E_{Fn} is caused by insufficient information about the level distribution in both materials.

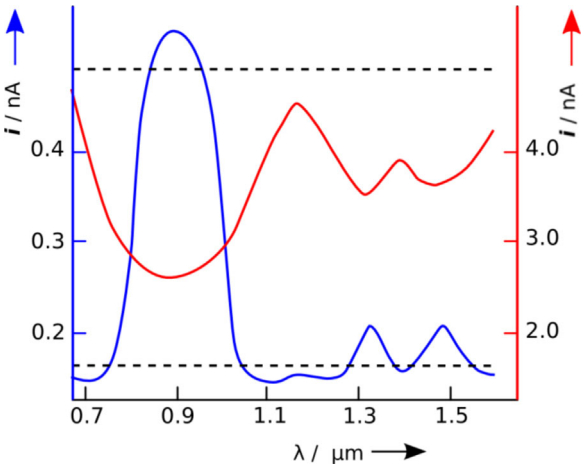

Figure 13 Photocurrent through a CdS single crystal (irradiated with a primary beam at 515 μm) as function of the wavelength of a secondary IR irradiation at low bias showing the typical quenching spectrum (in red), and at high bias when an anode-adjacent Böer domain is initiated showing infrared excitation (in blue) with maxima of quenching and excitation coinciding at the well known hole centers at wavelength 0.9, 1.2, 1.32, and 1.5 μm.

resulting in a hole density at the CdS/CdTe boundary of $p(\mathrm{CdTe_o}) = 1.25 \times 10^{10}\,\mathrm{cm^{-3}}$, resulting in $E_{Fp} - E_v = 0.54\,\mathrm{eV}$.

Figure 12 presents a first attempt to draw a to-scale model of the CdS/CdTe solar cell based on the dominant effect of the continuity of the dominant hole current that forces an adjustment of the interface dipole and causes a close joining of the valence bands. The unusual behavior of the quasi-Fermi level for holes in CdS is explained by the forced hole drift current in the junction-adjacent high-field domain. The quasi-Fermi levels for electrons in both materials are only indicated near each of the electrodes for reasons of insufficient experimental information of the defect structure in each. The Debye length $L_D = 1{,}205\,[\varepsilon_{stat} T \times 10^{15}/(10 \times 300p)]^{1/2}$ Å $= 15{,}000$ μm is much larger than the thickness of the CdS hence causing a close contact to the metal boundary with tunneling of holes to the metal.

The use of a copper-doped CdS layer directly adjacent to any p-type solar cell is also suggested with a consequent increase of the open circuit voltage approaching its theoretical value of the band gap of the emitter when extrapolated to 0 K [15].

4 Electrode-adjacent domains as tools With the electrode-adjacent domains present, this part of the crystal is space-charge-free and offers itself for investigation of the carrier density and mobility as function of the acting field and for transition near the quasi-Fermi-levels of minority carriers.

4.1 Change from n-type to p-type in photoquenching, the CdS is ambipolar In the normal (low field) and in the Böer Domain attached to the cathode the spectral distribution of the photocurrent shows the well known infrared Minima of the photocurrent IR quenching, indicating that the CdS is n-type and its carrier density decreases by increased recombination.

However, as soon as the applied voltage is increased above the value at the arrow shown in Fig. 11b, the spectral distribution is inverted and shows maxima at nearly the same positions (Fig. 13) indicating an inversion to p-type [16] that can extend through the entire part of the CdS [17]. Here the current is increased at the former "quenching minima" indicating an increased hole density for the drift current. A similar increase of the hole density was already observed by Palz and Ruppel and assigned to photovoltaic CdS [18].

4.2 Electron and hole densities as function of the electric field Since the anode adjacent super-high-field domain again lies near the singular point III, the carrier density and field must be constant, the current is saturated and must be described by drift only. The carriers in this domain must be holes, one has

$$j = j_p = e\mu_p pF.$$

The calculated hole densities shown in Fig. 14 are using this drift current argument. The hole density is larger in the anode-adjacent case by a factor of $(p/n = \mu_n/\mu_p) \times (E_{II}/E_{III}) = (300/50) \times (85/125) = 4$. This factor was used to determine the right side of the scale for holes in Fig. 13. The entire crystal is now in the third stable conduction state. Since this state is in practical application of CdS as a partner of the CdS/CdTe solar cell, we will call this in contrast to photoconducting CdS, the third state as photovoltaic CdS [19] state.

The entire carrier density of the homogeneous CdS can be obtained through such electrode-adjacent domains using various light intensities or virtual cathodes as described earlier [20] and is shown in Fig. 14. It is the electron density as function of the field below the minimum shown in red and the hole density above the minimum shown in green.

One concludes that with super-high-field domains above $100\,\mathrm{kV\,cm^{-1}}$, the gold anode becomes hole blocking and

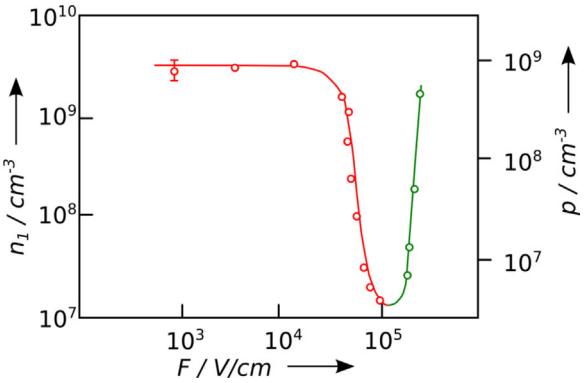

Figure 14 Carrier density (electron density below the minimum of the field and hole density above 100 kV cm^{-1}) as a function of the electric field, calculated from the drift current and the domain field, using the tabulated mobilities.

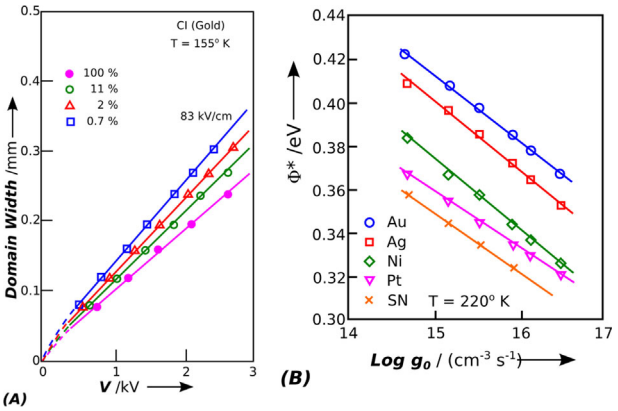

Figure 15 (a) High-field domain width as function of the bias for different light intensities for a gold contact, showing an increasing domain field at decreasing light intensities (given in the figure margin). (b) The work function decreases as function of the optical generation rate, shown for different blocking metal contacts.

stabilizes the third thermodynamic stable photovoltaic state of CdS.

4.3 Determination of the work function as function of the optical excitation Electrode-adjacent domains are determined by the work function of blocking contacts and thereby permit a closer analysis of the contact to CdS interface by shifting the space charge region away from the cathode to the bulk-side end of the domain. This allows a closer look at the thin space charge region between the metal-CdS interface that determines the actual height of the barrier before the high-field domain starts (we will do this in Section 4.4 below). This provides a more precise determination of the dependence of the work function on the photoconductivity of the adjacent CdS.

Since electrode-adjacent domains convert a blocking contact into a neutral contact, one is able to now measure sensitive changes of this "effective work function" with the optical excitation of CdS in a wide range of wavelengths. The experiments have shown that this work function decreases typically by 60 meV with an increase of the light intensity by two orders of magnitude (as is shown in Fig. 15a) [21]. Different blocking metals show a similar light intensity dependence (Fig. 15b). For every metal, a different CdS crystal (though of similar doping) had to be used. The similarity of the results given in Fig. 15b indicate that the light intensity dependence is not drastically influenced [22] by some differences in the defect structure of the CdS [23].

4.4 The spread of the quasi-Fermi levels and the effective work function The electrode-adjacent domains are an ideal means to spread the quasi-Fermi level to a precise value by adjusting the light intensity and then freezing this state while working within the electrode-adjacent high-field domain state. This all can be best explained by looking at a this slab starting from a blocking Schottky contact with a developing depletion space charge region and increasing field, until it reaches field quenching causing now a diminishing space charge, until it is

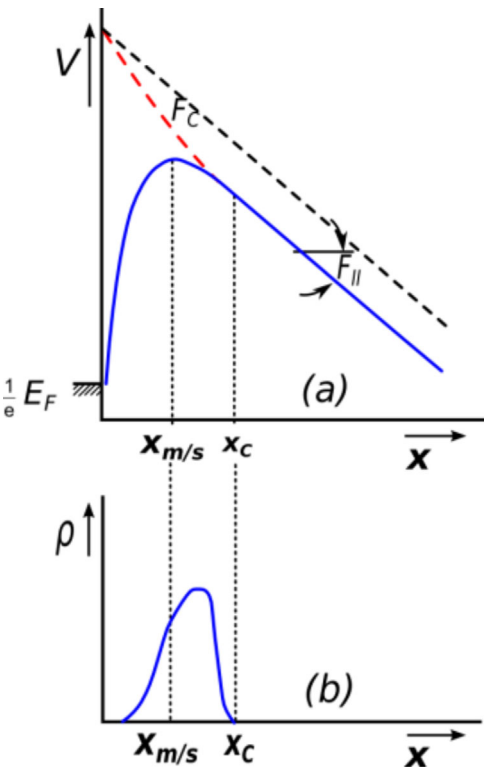

Figure 16 Potential and space charge distribution (schematically) between the Schottky barrier and the high-field domain starting at x_c. For the first part, the potential is determined by the image force, followed by the space charge, determined by depletion of electrons from donors and increases as the distance from the cathode increases, with the potential maximum at the boundary $x_{m/s}$. With increasing distance from the boundary the field increases . When it reaches the field-quenching range, more and more holes are excited to start compensating the space charge. When compensation is completed at x_c, the high-field domain starts.

completely compensated and the high-field domain starts (Fig. 16).

The region of a few Debye length thickness between the metal surface and x_c determines the actual work function. This is much more defined than in an ordinary crystal at which this potential maximum that defines the critical energy of electrons necessary to escape the metal depends on the doping, i.e., on the space charge that increases with applied voltage. That is taken into consideration by the conventional calculus of the characteristics. Here the conditions are much more precisely defined, and therefore, we like to call the resulting measurable work function the effective work function.

4.5 Small signal lock-in methods In this region, the quasi-Fermi levels are precisely spread and are constant in the entire high-filed domain since it is space-charge free and remain in this state as long as the light intensity is not changed. Small (sinoidal changes) can modulate the position of the quasi-Femi level and provide an ideal opportunity to measure transition coefficients with the well-known lock-in techniques. This has not yet been done but is a challenging opportunity for others to follow.

4.6 Vanishing space-charge as a means to measure the undisturbed spectral distribution of defect levels Defect levels are usually broadened by the field distribution in their neighborhood caused by space charges. In contact-adjacent high-field domains this is no longer the case, and very sharp levels may appear. An example is given in the following section (Fig. 17). The vanishing space charge described here with the example is one more case of vanishing interactions like in superconductivity where the interaction of electrons with phonons disappears, or in lasers where the interaction of photons with phonons disappears.

4.7 First observation of a strong electron quenching signal probably indicating why CdS cannot be doped p-type When, with an anode-adjacent domain present, the entire un-doped CdS crystal is exposed to infrared illumination only, then the conductivity maxima at 0.9, 1.3, 1.45 μm appear again, however, with an extremely sharp and deep minimum at 1.05 μm (see Fig. 17).

Such an inverted electron quenching with such sharp minimum is highly remarkable since it points to a deep tightly bond level close to the center but slightly above the middle of the band gap. It is not observed in optical absorption with such a discrete feature in a spectral distribution of the extrinsic range with light induced modulation of absorption spectroscopy [24]. However, it could be indicative as an intrinsic center that prevents doping-induced p-type, probably due to forced intrinsic compensation.

5 Summary It is shown that a benign *j–V* characteristic can contain a wealth of information when aided by the determination of the field distribution that shows in a copper-doped CdS with a blocking cathode electrode-adjacent high-field domains. These domains present two

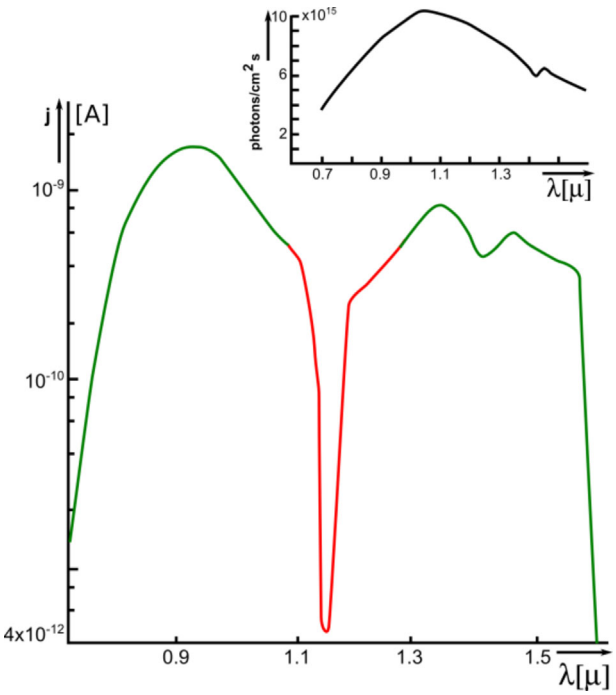

Figure 17 Spectral distribution of the p-type photoconductive undoped CdS crystal with gold electrodes while an anode-adjacent hyper-high-field domain is present [17]. The deep minimum is shown in red, indicating an electron signal from quenching imbedded in the hole excitation spectrum shown in green. The insert shows the spectral output of the monochromator indicating not such anomaly in the response.

new thermodynamic stable states of conductivity and characterize the model substance CdS as ambipolar. It is n-type in the normal, low-field state, and in the cathode-adjacent high-field domain state, and it is p-type in the anode-adjacent ultra-high-field domain state. Within these domains, the CdS is space-charge free and its conductivity is determined by drift alone, that make the determination of the carrier density and mobility as function of the acting field easy. It also separates the cathode to determine unambiguously the effective work function and measure its dependence on the light intensity. It provides a means to spread the quasi-Fermi levels throughout the crystal in a well defined way by the light intensity and offers access to the transition coefficients of electrons to trap levels at these quasi-Fermi levels by lock-in techniques. It permits the detection of a defect level spectrum that is undisturbed by the field broadening due to space-charge effects. It permitted already the discovery of a very distinct electron level in a highly purified CdS platelet that may be responsible for not permitting the CdS to become doped p-type.

References

[1] K. W. Böer and U. Kümmel, Vorprozesse des elektrischen Durchschlages in CdS Einkristallen, Z. angew. Physik **12**, 241–244 (1960).

[2] E. Schöll, Non-Equilibrium Phase Transitions in Semiconductors (Springer, Berlin, 1987);
M. P. Shaw, V. V. Mitin, E. Schöll, and H. L. Grubin, The Physics of Instabilities in Solid State Electronic Devices (Plenum Press, New York, 1987);
E. Schöll, Non-Linear Spatio-Temporal Dynamics and Chaos in Semiconductors (Cambridge University Press, Cambridge, 2001);
E. Schöll, Pattern formation and time-delayed feedback control at the nanoscale, in: Non-Linear Dynamics in Nano Systems, edited by G. Radons, B. Rumpf, and H.-G. Schuster (Wiley-VCH, Weinheim, 2010), pp. 325–367.
[3] K. W. Böer, H.-J. Hänsch, and U. Kümmel, Methode zum Sichtbarmachen von Leitfähigkeitsinhomogenitäten in Halbleitern, Naturwissenschaften **45**(19), 460 (1958).
[4] Klaus Thiessen introduced this term at the Semiconductor Session of the March Meeting of the German Physical Society in 2011 and it was accepted by all present, see: K. Thiessen, Böer Domains, Phys. Status Solidi B, DOI 10.1002/pssb.201046605 (2011) (Supporting Information).
[5] K. W. Böer and P. Voss, Stationary high-field domains in the range of negative differential conductivity in CdS single crystals, Phys. Rev. **171**, 899–911 (1968).
[6] The gold electrodes are evaporated on opposite site of the platelet to avoid glide discharge at higher applied voltages.
[7] K. W. Böer, The importance of gold-electrode-adjacent stationary high-field domains for the photoconductivity of CdS, Ann. Phys. (Berlin) **527**, 378–395 (2015).
[8] K. W. Böer and P. Voss, Stationary anode-adjacent high-field domains in cadmium sulfide, Phys. Status Solidi. **28**, 355 (1968).
[9] Using green color for holes, it is an overlay of a (n,F,x) plot and a (p,F,x) plot.
[10] The round semi-circles are the electrodes, avoiding sharp spikes at the contact points. Neglect the crystal striation that are seen in the pictures; they have no influence on the field distribution.
[11] This current limitation stabilizes the high-field domain in the CdS.
[12] K. W. Böer, High-field domains in CdS adjacent to a junction in a p-type solar cell, J. Appl. Phys. **119**, 085703 (2016).
[13] There is recently a press release of a CdTe solar cell with 21% efficiency and V_{oc} = 0.876V, j_{sc} = 30.25 A/cm^2 and FF = 79.4%, however there is not sufficient other information to draw a band model to this improved cell: M. A. Green et al., Solar Efficiency Tables (Version 46), Prog. Photovolt. Res. Appl. **23**, 305–312 (2015).
[14] Assuming a 5% interface recombination (95% quantum-efficiency) and the current from the CdTe at the interface of 25 mA/cm^2 with 1 mA/cm^2 diverted to interface recombination.
[15] K. W. Böer, Patents applied in USA, Germany and China.
[16] K. W. Böer and J. J. Ward, New kind of field instability in CdS in the range of negative differential resistivity, Solid State Commun. **5**, 467 (1967).
[17] K. W. Böer and J. J. Ward, p-type photoelectric behavior in CdS in a high-resistive region near the anode, Phys. Rev. **154**, 757 (1967).
[18] W. Palz and W. Ruppel, Low wavelength photovoltage and photoconductive quenching in CdS single crystals, Phys. Status Solidi. **6**, K161–K164 (1964); Phys. Status Solidi. **15**, 649 (1966).
[19] The application of CdS as a cover layer to make CdTe a higher efficient solar cell has been pointed out earlier: K. W. Böer, J. Appl. Phys. **107**, 023701 (2010) and recently has been confirmed by field limitation between 32 and 35 kV/cm in the CdTe part of the cell by R. G. Dhere et al., Investigation of junction properties of CdS/CdTe solar cells and their correlation to device properties, Proc. 33rd IEEE Photovolt. Spec. Conf. (2008) pp. 1137–1141.
[20] K. W. Böer and W. E. Wilhelm, Artificial initiation of layer-like field inhomogeneities in CdS single crystals, Phys. Status Solidi **4**, 237 (1964).
[21] R. J. Stirn, K. W. Böer, G. A. Dussel, and P. Voss, CdS-Metal Workfunction at Higher Current Densities, Proc. Third Photoconductive Conf. (Pergamon Press, Oxford, 1971), p. 389.
[22] An influence of the space charge region very close to the cathode is however expected – for more details see Section 4.5.2.
[23] R. J. Stirn, G. A. Dussel, and K. W. Böer, CdS metal contact at higher current densities, Phys. Rev. B **7**(4) 1433–1443 (1973);
G. A. Dussel, K. W. Böer, and R. J. Stirn, Photoconductor metal contact at higher densities, Phys. Rev. B **7**(4), 1443–1454 (1973).
[24] K. W. Böer, Light-induced modulation of absorption (LIMA) of CdS single crystals, Z. Naturforschung **24a**, 1306–1310 (1969).